Chapter 2
Fiber Optic Interferometric Devices

Utkarsh Sharma and Xing Wei

2.1 Introduction

Fiber optic interferometry can be broadly explained as the techniques that utilize the fundamental principles of optical interference to measure physical sample properties or detect changes via sensing systems that are partially or completely realized using fiber optic components. While the field of optical interference dates back to second half of seventeenth century, the advent of fiber optic interferometry technology is rather recent as it stemmed out of advances in the fiber optics in late 1970's and early 1980's. In the next two sections, we will briefly review the major advancements made in the field of optical interferometry and fiber optic interferometric devices.

2.1.1 Developments in Optical Interferometry: A Journey towards Understanding Light

Historically, the experiments based on optical interference over the last three centuries have played a key role in helping the physicists and scientists to make breakthrough advancements in Physics and led to wide range of applications involving highly sensitive metrology and sensing [1–3]. One of the unique advantages that the phenomenon of optical interference offered to the physicists was the capability to realize experimental optical setups and analyze the results that could be used to either verify or question their hypothesis and theories. The understanding of fundamentals of light and optical interference has come a long way since physicists first started exploring this subject matter more than three centuries ago. In one of the earliest experiments dating back to 1665, it was

U. Sharma (✉) · X. Wei
Carl Zeiss Meditec, Inc., 5160, Hacienda Drive, Dublin CA-94568, USA
e-mail: Utkarsh.1980@gmail.com

J. U. Kang (ed.), *Fiber Optic Sensing and Imaging*,
DOI: 10.1007/978-1-4614-7482-1_2,

F. M. Grimaldi's careful observations regarding the phenomenon of diffraction that first hinted at the wave-nature of the light. R. Hooke and C. Huygens furthered the wave theory of light but it was Newton's assertion of corpuscular theory of light that found broader acceptance for most of the seventeenth and eighteenth century. It was the remarkable contributions of E. Young, A. Fresnel and J. C. Maxwell that emphatically put the wave theory of light in the forefront again in the nineteenth century. Finally, in the era of the birth of modern physics and quantum mechanics in the twentieth century, the path-breaking works of M. Planck, A. Einstein, L. deBroglie, N. Bohr, W. Heisenberg and other notable physicists helped in establishing the wave-particle dual nature of light. It may be fitting to say that mankind's continually evolving understanding of the fundamentals of light and phenomenon such as optical interference has mirrored with the key advances made in the field of Physics over the last three centuries.

2.1.2 Fiber Optic Interferometry

While the impact of optical interferometry on modern physics cannot be overstated, it has been the advancements in the fiber optic interferometry technology that can be credited for utilizing this phenomenon for a wide range of commercial and industrial applications including strain sensors for structural monitoring, medical imaging, remote sensing and precise measurement applications to name a few [4–6]. There have been three critical factors that have been instrumental towards development of this technology. Firstly, it was the invention of laser that provided a high intensity light source with strong spatial and temporal coherence properties. Secondly, it was the advancements in optoelectronics industry that facilitated development of optical detectors to realize sophisticated low noise detection techniques to record optical interference effects with high sensitivity. And finally, it was the development of low loss single mode fibers that made it possible guide light in a flexible fiber optic waveguide and realize compact, low-cost, robust and versatile fiber optic interferometers that would otherwise be impractical to achieve with bulk-optic components.

Two of the major contributions of fiber optic interferometry have been in fiber optic sensors and fiber optic devices. In this chapter, we will largely focus on fiber optic sensors and its applications.

2.1.2.1 Advantages of Fiber Optic Technology

There are some unique advantages of fiber optics technology that make it especially attractive for sensing applications [5].

1. Compact and lightweight: Fiber optic interferometers and sensors can be made highly compact and hence find use in airborne and space-based sensing applications.
2. High accuracy and sensitivity compared to typical mechanical or chemical based sensors.
3. Flexibility for customized applications: Single mode fibers (SMF) provide a loss-less and flexible optical wave-guide for transmission, delivery and collection of optical signals. For example, one can use a flexible fiber to deliver or collect light from internal body organs by integrating an optical fiber with an endoscope. One can also utilize the nearly loss-less transmission properties of SMFs for remote sensing operations.
4. Silica material properties: Optical fibers are made from silica (glass) and hence carry some inherent advantages such as usability in harsh, high temperature and rugged environments, and immunity to electromagnetic interference. Silica is also a chemically passive material and hence it is not affected by corrosive factors that might be present in the environment.
5. Multiplexing capabilities that allow distributed sensing applications.

2.1.2.2 Fiber Optic Interferometry Based Sensing: Technology Trends and Applications

Fiber optic sensor technology was touted to be a huge breakthrough in 1980's and early 1990's. Although it led to several successful commercial applications and its impact on research and specialized engineering applications has been invaluable, it has still failed to achieve the widespread commercial penetration in the sensors market that it had once promised. The main reason for this failure is the stiff competition it has faced due to existence of low cost conventional alternatives such as electronic/mechanical or chemical sensors. The sensors industry is highly fragmented with various independent market sectors where each has very specialized needs [6]. Although fiber optic technologies could offer higher resolution and precision, such high sensitivities are often not required for most commercial applications.

It was the steep growth of telecommunication industry in the 1990's that fueled the research and development in fiber optics technology and led to availability of less costly, efficient and more sophisticated fiber optic components. However, the cost of fiber optic sensor technology still needs to be reduced significantly to offer a compelling incentive to sensors industry for adoption of the newer technology. The prices of fiber optic and optoelectronic components such as laser diodes and SMFs have seen a steep decrease by a factor of around hundred-folds over the last 30 years [5]. It is likely that this downward trend in prices will continue as the technology matures further, and this may open up newer possibilities for optical fiber sensor technology.

There is also an alternative route towards progressive commercial success for fiber optic sensor technology. The key to this approach would be to identify and develop niche applications that can benefit from the unique advantages of the fiber optic sensors. Environmental and atmospheric monitoring, industrial chemical processing, advanced manufacturing processes, biotechnology, and defense are some of the areas that can utilize the improved performance of the newer technology. With increased emphasis on monitoring the environmental changes, fiber optic sensors could play a pivotal role in real-time measurements of pollutant levels and contamination in the environment. The multiplexing and distributed sensing capabilities of fiber optic sensors make them an excellent candidate for structural health monitoring in airborne and satellite applications where weight is a major consideration. It can also be used to remotely monitor chemical processes in otherwise rugged and hazardous conditions. In medicine, fiber optics has been found extremely useful in realizing optical imaging techniques such as optical coherence tomography and delivering therapeutic light into an internal organ via optical fiber conduit. Overall, the field of fiber optic interferometry is bound to prosper and have a wider commercial impact in future as the technology evolves and finds newer applications.

In the following section, we will discuss the basic fundamentals of fiber optic interferometry and sensors. In Sect. 2.4, we will review basic principles of operations of some of the selected fiber optic components that are routinely used to realize fiber optic interferometric sensors and devices. In Sect. 2.3, several interferometric architectures will be covered along with a few selective examples of applications that use these interferometers.

2.2 Fundamentals of Optical Interferometry and Fiber Optic Sensors

In this section, we will review the basic fundamentals about the optical interference, and generic descriptions of fiber optic sensors. In the topics describing fiber optic concepts and applications, the analysis will be limited to single mode optical fibers for the scope of this chapter.

2.2.1 Optical Interference and Wave Representation of Light

As per the scalar wave model, monochromatic light constitutes of oscillating electric and magnetic field components that can be mathematically represented by the wavefunction $\psi(r,t)$, where it is a function of time, t and spatial position, $r = (x, y, z)$. As derived from Maxwell's equations in the earlier chapter, the light wavefunction satisfies the following scalar wave equation in vacuum,

$$\nabla^2\psi(r,t) = \frac{1}{c^2}\frac{\partial^2\psi(r,t)}{\partial t^2}, \tag{2.1}$$

where ∇^2 is the Laplacian operator, and c is the speed of light in vacuum. Any function that satisfies the above equation could be a possible representation of optical waves. A characteristic property of the scalar wave equation is that it is linear, and hence the principle of superposition can be applied if there is an interaction of two or more wavefunctions. If the two optical fields, $\psi_1(r,t)$ and $\psi_2(r,t)$, have an overlap then the resulting optical field is given by the linear superposition of the two waves as shown in the following equation:

$$\psi_{Tot}(r,t) = \psi_1(r,t) + \psi_2(r,t). \tag{2.2}$$

It is often mathematically convenient to represent the light waves as complex fields, although the electric or magnetic fields that carry the energy are represented by the real part of this complex field. Monochromatic plane wave solution is often used to describe various fundamentals of light as it is one of the simplest solutions for the scalar wave equation. A monochromatic plane wave can be mathematically represented as following:

$$\begin{aligned}\psi(\vec{r},t) &= E_0 \exp\left(i\left(\vec{k}.\vec{r} - 2\pi\upsilon t\right)\right)\\ &= E_0 \exp\left(i\left(k_x x + k_y y + k_z z - 2\pi\upsilon t\right)\right),\end{aligned} \tag{2.3}$$

where E_0 is the field amplitude, $\vec{k}$ is the propagation wavevector, and υ is the frequency of light. Often in a simplified form, a plane wave propagating in the z direction is represented as $E_0 \exp(i(kz - \omega t))$, where $\omega(= 2\pi\upsilon)$ is the angular frequency of the light. In context to this chapter, a modified plane wave based solution is also quite suitable to model light propagation in single mode fibers when weakly guiding approximation is used [Chap. 1].

2.2.1.1 Interference of Monochromatic Planar Waves

The resulting electric field due to interference of two co-propagating plane waves of the same frequency can be given as:

$$E_{Tot} = E_1 \exp(i(kz - \omega t + \phi_1)) + E_2 \exp(i(kz - \omega t + \phi_2)), \tag{2.4}$$

where, E_1, E_2 and ϕ_1, ϕ_2 are the amplitudes and the phases of the two waves respectively. The frequency of optical light is very high ($\sim 10^{14}$ Hz) and hence one can only detect the intensity of the light using optical detectors. The intensity is proportional to the time-averaged value of squared electric field: $I\alpha\langle E.E^*\rangle$ (refer Chap. 1 for more details). The intensity of the resulting field in Eq. (2.4) at the detector can be given as follows:

$$\begin{aligned} I_{Tot} &= \langle (E_1 + E_2).(E_1 + E_2)^* \rangle = |E_1|^2 + |E_2|^2 + 2\mathrm{Re}\left(E_1 E_2^*\right) \\ &= |E_1|^2 + |E_2|^2 + 2|E_1||E_2| cos(\phi_1 - \phi_2) \end{aligned} \tag{2.5}$$

Hence, the resulting intensity due to interference of two waves is simply not the sum of the individual intensities but is rather given by:

$$I_{Tot} = I_1 + I_2 + 2\sqrt{I_1 I_2} cos(\phi_1 - \phi_2). \tag{2.6}$$

It should be noted that the effective phase difference ($\phi_1 - \phi_2$, in this case) plays an important role and determines if it is a constructive ($\phi_1 - \phi_2 = 2n\pi$; $n = 0, \pm 1, \pm 2 \ldots$) or destructive interference ($\phi_1 - \phi_2 = (2n-1)\pi$; $n = 0, \pm 1, \pm 2 \ldots$). If two identical optical waves (assuming zero phase offsets, i.e. $\phi_1 = \phi_2$) undergo different path lengths before interference occurs, then it will result in phase difference, $\Delta\phi = k(z_1 - z_2) = k\Delta z$, where Δz is the path difference between two waves. If the phase difference changes continuously, it will result in interference fringes and the measured intensity will vary from a maximum of $I_{\max}\left(= I_1 + I_2 + 2\sqrt{I_1 I_2}\right)$ to a minimum of $I_{\min}\left(= I_1 + I_2 - 2\sqrt{I_1 I_2}\right)$. A useful parameter of interest is the fringe visibility contrast or fringe modulation depth and is defined as: $\dfrac{I_{\max} - I_{\min}}{I_{\max} + I_{\min}} = \dfrac{2\sqrt{I_1 I_2}}{I_1 + I_2}$.

2.2.1.2 Interference of Planar Waves of Different Frequency

In the last sub-section, we discussed the interference between two waves with same frequency but different optical path length or phase difference. Another important interference phenomenon is the resulting electric field due to interference of plane waves of the different frequency. This mathematical analysis is especially useful because in reality light waves are not strictly monochromatic but have a finite spectral bandwidth. Having a finite bandwidth allows the ability to modulate the field amplitude. Availability of high speed optical modulators (electro-optic and acousto-optic) make it possible realize many useful technologies that have had far reaching impact in fiber optic industry. Mathematically the sum of two waves of equal amplitude but with different angular frequency can be represented as following (assuming zero phase offsets for simplicity, i.e. $\phi_1 = \phi_2 = 0$):

$$\begin{aligned} E_{Tot} &= E_0 \exp(i(k_1 z - \omega_1 t)) + E_0 \exp(i(k_2 z - \omega_2 t)) \\ &= E_0 \exp(i(k_1 z - \omega_1 t)) + E_0 \exp(i((k_1 + \Delta k)z - (\omega_1 + \Delta\omega)t)), \end{aligned} \tag{2.7}$$

where the angular frequency and the propagation wavevector of the two waves differ by $\Delta\omega$ and Δk, respectively. If we simplify for the real part (electric field value) of the Eq. (2.7) above then we get:

$$\begin{aligned}\mathrm{Re}(E_{Tot}) &= 2E_0\cos\left(\left(k_1+\frac{\Delta k}{2}\right)z-\left(\omega_1+\frac{\Delta\omega}{2}\right)t\right)\cos\left(-\frac{\Delta k}{2}z+\frac{\Delta\omega}{2}t\right)\\ &= E_{Mod}(t)\cos\left(\left(k_1+\frac{\Delta k}{2}\right)z-\left(\omega_1+\frac{\Delta\omega}{2}\right)t\right),\end{aligned} \tag{2.8}$$

where the resulting wavefield has a modulated amplitude $E_{Mod}(t) = 2E_0\cos\left(-\frac{\Delta k}{2}z+\frac{\Delta\omega}{2}t\right)$.

The resulting intensity measured by detector has modulations with a beat frequency, $\Delta\omega$, as shown in the equation below:

$$\begin{aligned}I_{Tot} &= \langle(E_1+E_2).(E_1+E_2)^*\rangle = |E_1|^2+|E_2|^2+2\mathrm{Re}\left(E_1E_2^*\right)\\ &= 2I_0(1+\cos(-\Delta kz+\Delta\omega t)) = 4I_0\cos\left(\frac{-\Delta kz+\Delta\omega t}{2}\right)^2.\end{aligned} \tag{2.9}$$

This result has a huge significance as beat frequencies can be orders of multitude smaller than the optical frequency ($\sim 10^{14}$ Hz) which cannot be detected using optoelectronic detectors. Instead one can rely on measurement of beat frequency (typically kHz–GHz range) for highly sensitive phase measurements. Figure 2.1 shows linear sum of two monochromatic waves of different frequency and different amplitude. It should be noted that the resulting modulation depth is not the maximum because the two waves have different amplitude.

Note: It must be noted that interference or linear superposition of the scalar electric field applies only if the two waves have same polarization. Otherwise, the addition of the two differently polarized light waves would result in an output field of new polarization. Another important point to note is that both temporal and spatial coherence are required for two fields to manifest interference effects. Spatial coherence is a measure of correlation between electric field or wavefunctions at two different positions in space. Temporal coherence is a measure of

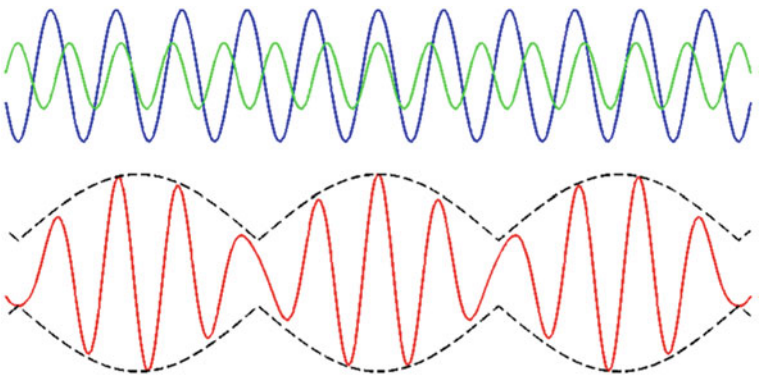

Fig. 2.1 Superposition of two monochromatic waves of different frequency and amplitude (in *blue* and *green*). The resulting electric field is given by the *red* graph below, with amplitude modulation showed with *dashed black lines*

correlation or predictable phase relationship between fields or wavefunctions observed at different points in time. As per the mathematical definition, monochromatic plane waves that we have used so far in our analysis have infinite coherence time and coherence lengths.

2.2.1.3 Quasi-monochromatic, Polychromatic, and Broadband Light

Monochromatic plane wave representation is a great tool to understand some of the basic fundamentals of wave theory of light [2, 3]. However, in reality, there is no such thing as a monochromatic plane wave because a truly monochromatic plane wave has infinite energy and infinite time duration (time from $-\infty$ to $+\infty$). In fact, all the travelling light waves that carry energy have finite bandwidths and hence for simplicity, we would call it polychromatic light. Polychromatic waves can be expressed by using weighted sum of monochromatic waves of different frequencies using the famous principle of superposition. The use of Fourier methods greatly simplifies the representation of broadband light. For example, an arbitrary wavefunction, $E(t)$, can be defined for a given location (say at $z = 0$) using the superposition integral of monochromatic waves of different frequencies, amplitude and phases as shown in the equation below:

$$E(t) = \frac{1}{2\pi} \int_{-\infty}^{\infty} \tilde{E}(\omega) \exp(-i\omega t) d\omega. \tag{2.10}$$

Here $E(\omega)$ can be obtained by carrying out the Fourier transform as shown below:

$$\tilde{E}(\omega) = \int_{-\infty}^{\infty} E(t) \exp(i\omega t) dt = F.T.\{E(t)\}. \tag{2.11}$$

The spectrum of the wavefunction, $E(t)$, is defined as the absolute value of the square of the Fourier transform of the wavefunction: $S(\omega) = |F.T.\{E(t)\}|^2 = |E(\omega)|^2$.

2.2.2 Phase and Group Velocity

The concept of group velocity and optical path delay is inherently central to any practical interferometric setup. So far we have described monochromatic waves that travel in vacuum with the phase velocity, $v_{Ph} = \frac{\omega}{k} = c$. When the waves travel in a dispersive medium with refractive index n, the phase velocity is given as: $v_{Ph} = \frac{c}{n}$. We have already discussed that monochromatic waves are ideal

representations and hence do not carry any energy. For a monochromatic wave, this is often called phase velocity, and in vacuum, EM waves of different frequency travel with the same phase velocity, i.e. of light. In reality, however, energy is carried by wave packets or wave pulses and any media of propagation has dispersion (see Chap. 1). Unlike, monochromatic waves that have indefinite extent in time, a wave packet consist of a localized wavefunction (spatial or temporal) that travels with a group velocity $\left(v_g = \frac{\partial\omega}{\partial k}\right)$ in a dispersive medium. Figure 2.2 shows the resulting wave packet as a result of superposition of multiple monochromatic waves of variable frequency and amplitudes. In reality, a light pulse of localized energy is made up of continuum of frequencies (that essentially can be explained by the sum of Fourier frequencies of the light pulse). In the Fig. 2.2, we can see that even the discrete number of wavelengths or frequencies can add up to form a modulated electric field envelope or wave packet.

In Sect. 2.2.1.2, we saw an interesting result that when two monochromatic waves of different frequency superimpose, it results in modulated electric field amplitude. One of the key insights from this result is that superposition of many monochromatic light waves with varying frequencies around a central frequency can result in a localized light wave packet or a light pulse. In Eq. (2.8), the simplified expression of the combined waves depicted a monochromatic wave with average wavevector and frequency $\left(\bar{k} = k + \frac{\Delta k}{2};\ \&\ \bar{\omega} = \omega + \frac{\Delta\omega}{2}\right)$, but with amplitude modulation. If we look at the modulated envelope, we realize that it has a phase of its own and it travels with a group velocity of:

$$v_g = \frac{\Delta\omega}{\Delta k} = \frac{\partial\omega}{\partial k} \tag{2.12}$$

Hence for propagation of light in any optical media, the group refractive index (n_g) is defined as: $n_g = \frac{c}{v_g}$. It must be noted that group refractive index should not be confused with the refractive index (n), which is defined as: $n = \frac{c}{v_{Ph}}$.

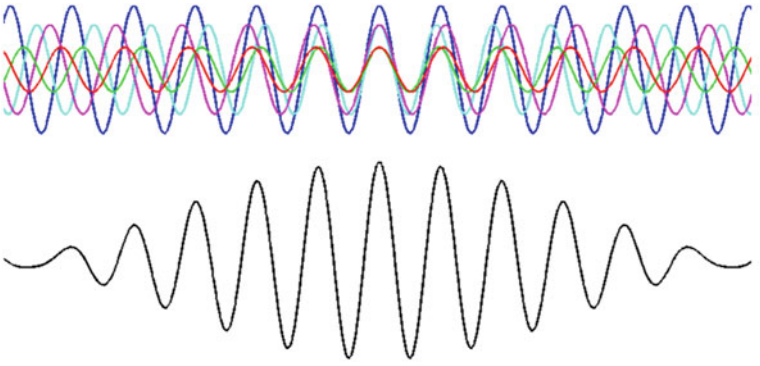

Fig. 2.2 Superposition of multiple monochromatic waves of varying frequency and amplitude results in formation of a wave packet below (*black*)

When light travels through a fiber or any other optical media, the phase term of the associated electric field is modified as follows: $E_{out} = E_{in}\exp(ik_0nz)$, where n is the refractive index, k_0 is the wavenumber in vacuum, and z is the distance travelled in the media. One of the often used term in interferometry is the optical path length (OPL), which is described as the product of the physical distance travelled by an electric field and the refractive index of the medium ($OPL = nz$). A related and equally useful term is called optical path difference (OPD), which is described by the differential OPL between two light waves of the same origin, but that travelled through different media or different distances. OPD is often calculated in two beam interferometry and is given by: $OPD = n_1z_1 - n_2z_2$. For many applications in interferometry, it is often convenient to use the group refractive index to calculate the OPD or OPL.

2.2.3 Fiber Optic Interferometric Sensors

In a typical fiber optic interferometric sensor, the light is divided in at least two parts and at least one part of the light interacts with the measurand (a quantity or physical effect that is intended to be measured). The interaction of the measurand with the light field would result in a phase shift or phase modulation, which can be detected when the modified light field interferes with the reference light (Fig. 2.3). Fiber optic interferometric sensors typically offer high sensitivities due to several reasons including low propagation loss in fiber, and interferometric detection. As shown in Fig. 2.3, the light can be modified by multitudes of environmental perturbations or measurable quantities such as temperature, strain, heat, humidity, force, pressure, flow, acoustic, vibrations, acceleration, velocity, electric or

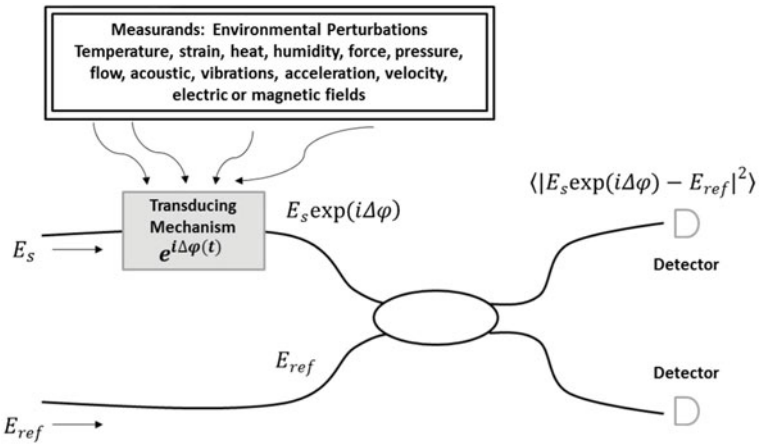

Fig. 2.3 Schematic to show a generic interferometric fiber optic sensor. Environmental perturbations such as temperature, strain, pressure etc. interact with the light field and impart a phase shift or modulation that can be analyzed by processing the interference term at the detector

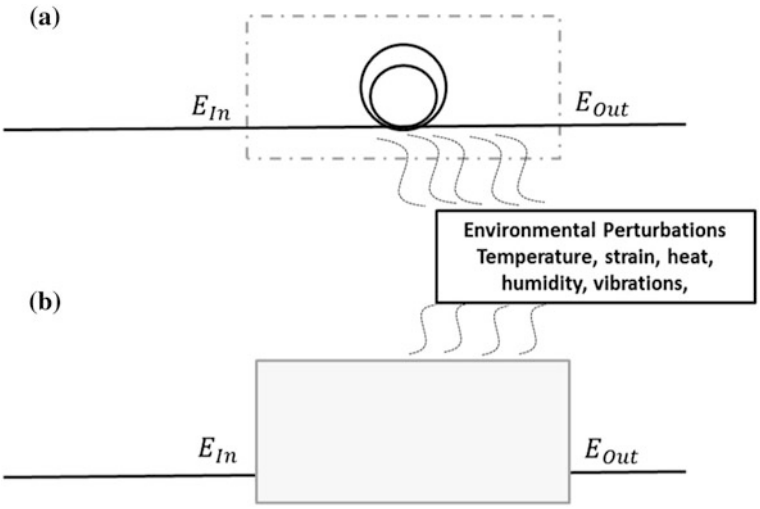

Fig. 2.4 Schematic to show a generic intrinsic and extrinsic fiber optic sensors. **a** intrinsic fibre sensors. **b** extrinsic fiber sensors

magnetic fields etc. These environmental perturbations interact with the electric field through a transducing mechanism and impart a change or modulation in the phase term: $\Delta OPL = \Delta(k_0 nz)$.

Broadly speaking, fiber optic sensors can be divided into two categories (Fig. 2.4):

- Intrinsic fiber sensors: The light is modified inside the fiber and the fiber itself acts as a transducer, in part or as a whole. Often the fiber is attached to a material that acts as a transducer in tandem with fiber. The intrinsic fiber sensors have the advantage of compact and efficient design with high sensitivity.
- Extrinsic or hybrid fiber sensors: The light is carried by a fiber to a location where the light is modified by environmental perturbations or measurand, and the modified light is then collected back by the same or another fiber and directed to a detector where it is processed and analyzed. One of the major advantages of the extrinsic fiber sensors is that the fiber acts as a flexible and rugged dielectric conduit of light and enables delivery and collection of light for measurement purposes, which otherwise would had been prohibitive due to harsh environmental conditions.

In the intrinsic fiber sensors, these environmental perturbations impart a change in the physical property of the fiber itself; such as temperature or strain induced changes in length or refractive index which in turn imparts a change in the optical phase of the light travelling through the fiber. On the other hand, extrinsic fiber sensors could have much wider range of applications because it is then feasible to expand the transducing mechanisms as the light is not necessarily confined within the fiber when interacting with the perturbation field.

2.3 Fiber Optic Interferometer Architectures

In this section, we will briefly discuss some of the common fiber optic interferometer architectures topologies and draw parallels with their bulk optic counterpart interferometer architectures. The four interferometer architectures are Michelson, Mach–Zehnder, Sagnac and Fabry–Perot interferometers. The goal for this section is to provide the reader with an overview of different architectures and a more detailed treatment for most of these designs is either provided in the later sections (Michelson and Mach–Zehnder interferometers in Sect. 2.4 of this chapter) or later in this book (see the chapter on Sagnac interferometer later in the book). In principle, any of the interferometric architecture (with the exception of Sagnac interferometer) can be alternatively realized to measure any of the physical properties. However, different architecture may present different design, cost and performance trade-offs and one or another architecture may be preferred depending upon the unique requirements of a specific application.

2.3.1 Michelson Interferometer

Michelson interferometer is probably the most commonly known optical configuration that is used for interferometry. One of the most significant applications of this interferometer was in the famous Michelson-Morley experiment that was carried out in 1887 to detect the relative motion of earth and aether in the universe. While the unexpected results of the experiments confounded scientists at the time, it was one of the key findings that inspired Einstein's special theory of relativity.

Figure 2.5 shows the typical schematics of bulk-optic and fiber optic realizations of Michelson interferometers. In a Michelson interferometer, an incident light field

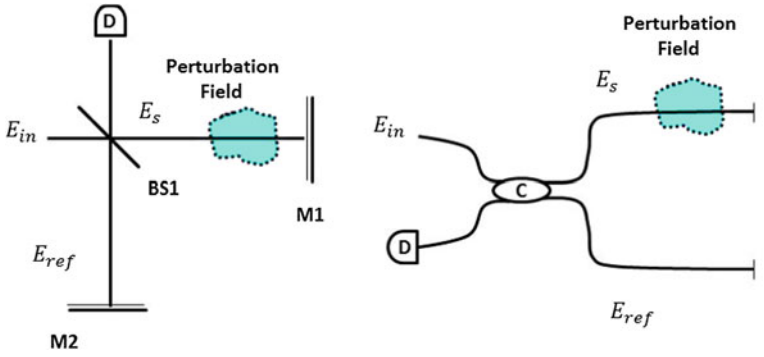

Fig. 2.5 Schematic design for bulk-optic (*left*) and fiber optic Michelson interferometer architecture. The electric fields, optical and fiber optic components shown in the figure are as follows: E_{in}: incident electric field; E_s: electric field in the sample arm; E_{ref}: electric field in the reference arm; *BS1*: beam splitter; *M1* and *M2*: mirrors; *C*: fiber optic coupler; and *D*: detector

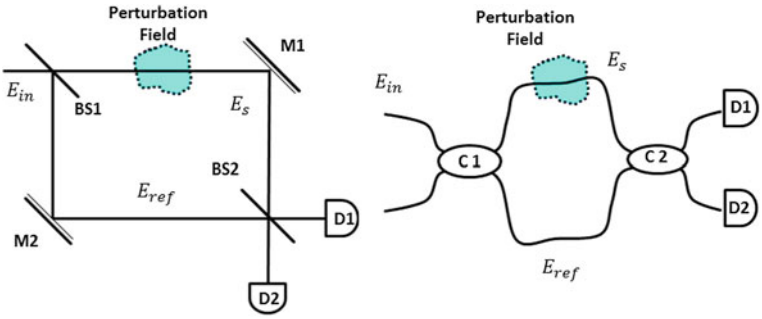

Fig. 2.6 Schematic design for a bulk-optic (*left*) and fiber optic Mach–Zehnder interferometer architecture

is divided into two parts (sample and reference) by a beam splitter or fiber optic coupler. The light in the reference and sample paths are reflected back and combined using the same splitter and the interference patterns of the two lights are measured using a detector. The light in the sample arm accrues perturbation field dependent phase shifts that can be measured using interference with the reference light.

2.3.2 Mach–Zehnder Interferometer

In a Mach–Zehnder interferometer, the incident light field is divided into two parts (sample and reference) by a beam splitter or fiber optic coupler. Unlike Michelson, the light in the reference and sample paths is not reflected; rather it is directed to a second splitter/combiner where the two lights combine and the interference patterns are measured using detectors (Fig. 2.6). In fact, if a Mach–Zehnder interferometer is cut in half and folded back, the topology will become similar to that of Michelson interferometer.

2.3.3 Fabry–Perot Interferometer

A Fabry–Perot (FP) interferometer of etalon consists of two reflective surfaces that are often parallel. The incident light is reflected back and forth and transmitted multiple times at the two partially reflective surfaces. The superposition of these multiply reflected and transmitted beams at the two surfaces results in interference effects that determine the transmission and back-reflected light characteristics of the light. Figure 2.7 shows various bulk-optic and fiber optic realizations for FP interferometers. The two examples corresponding to extrinsic and intrinsic fiber optic FP interferometers are also shown. In the intrinsic fiber optic FP sensor the reflective surfaces inside the fiber can be created by micro-machining, fiber Bragg gratings (FBG), or thin film deposition.

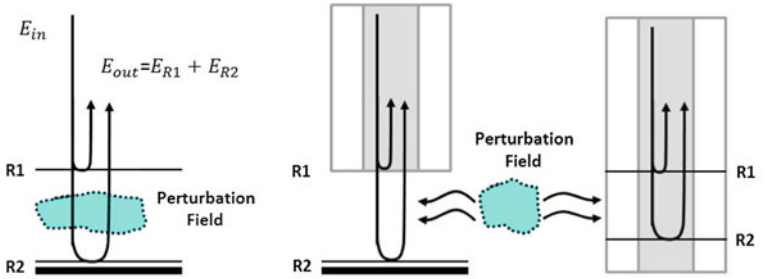

Fig. 2.7 Schematic design for a bulk-optic (*left*), extrinsic fiber optic (*middle*), and intrinsic fiber optic (*right*) Fabry–Perot interferometer architecture. *R1* and *R2* are the two reflective surfaces forming the Fabry–Perot cavity

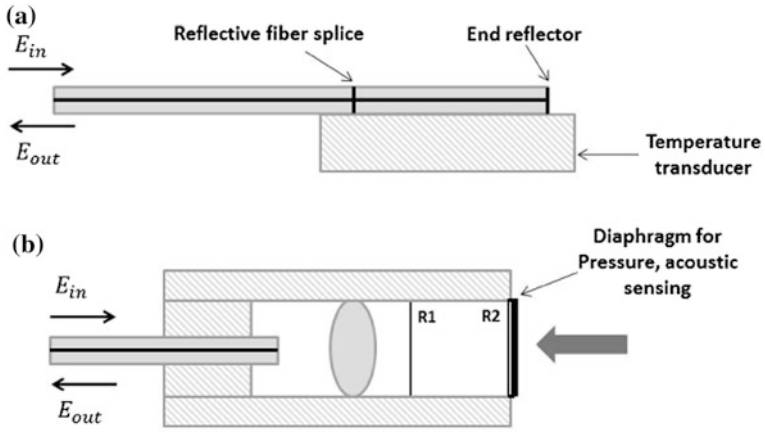

Fig. 2.8 **a**. Intrinsic FP interferometer based sensor for thermal measurements. **b**. Extrinsic FP interferometer based sensor for pressure acoustic sensing

In Sect. 2.2.3, we discussed that environmental perturbations could modify the medium of propagation of light and result in phase shifts that is proportional to effective change in *OPL* as shown here: $\Delta\phi = \Delta(nk_0z) = k_0z\left(\Delta n + \frac{n\Delta z}{z}\right)$. Several environmental perturbations such as temperature, pressure, strain and acoustic waves could impart these phase shifts via interaction with fiber or external medium. For example, Fig. 2.8a shows an intrinsic fiber optic temperature sensor based on FP interferometer. Here the composite material attached to the fiber introduces temperature dependent strain to the fiber, thereby resulting in phase shifts. Figure 2.8b shows another FP interferometer based implementation that can be used to measure acoustic waves or pressure changes. The diaphragm with a reflective surface on one side acts as a transducer which results in displacement with respect to pressure or acoustic changes.

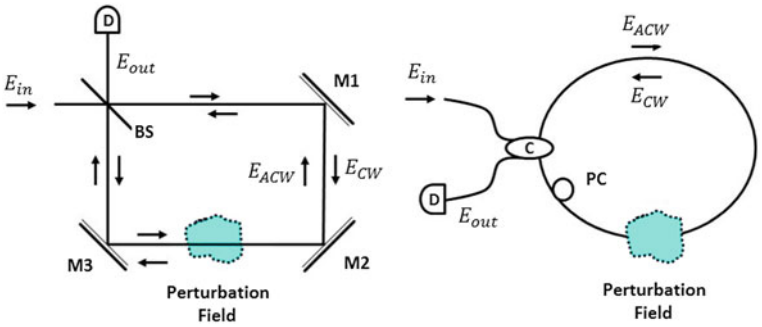

Fig. 2.9 Schematic design for a bulk-optic (*left*), and intrinsic fiber optic (*right*) Sagnac interferometer architecture. E_{CW} and E_{ACW} are the electric field traveling in the clockwise and anticlockwise direction in the Sagnac ring or loop

2.3.4 Sagnac Interferometer

In Sagnac or ring interferometer, the incident light field is split into two parts. While the path travelled by the two beams is the same, the two beams travel in opposite angular directions (i.e. clockwise and anti-clockwise). After completing the loop trajectory, the two beams combine at the point of entry and undergo interference (Fig. 2.9). Because the two beams move in opposite angular directions, the interference signal at the coupler is highly sensitive to the angular motion of Sagnac loop itself. Sagnac interferometers have found applications in fiber optic gyroscopes and a more detailed discussion on theory and applications will be provided in the later chapter.

2.4 Basic Operation Principles of Fiber Optic Components and Assemblies

It is important to understand the basic operation principles of some of the selected fiber optic components as majority of fiber optic sensors and interferometric setups can be realized using these components. This section focuses on providing the basic mathematical tools to model these components for interferometry applications.

2.4.1 Ideal 2 × 2 Fiber Optic Couplers

A very basic fiber optic component is a 2 × 2 fiber optic coupler that has two input ports and two output ports, each port being a single-mode fiber that supports only the LP01 mode of light at the wavelength of interest (Fig. 2.10). The "single-mode"

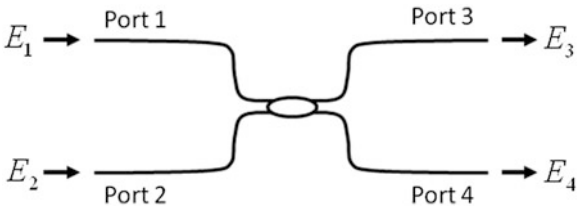

Fig. 2.10 Coupling of light through a 2 × 2 fiber optic coupler

fiber actually supports two degenerate modes of orthogonal polarizations. But for simplicity the polarization effects are ignored for the moment. The light signals entering the two input ports are mixed in the coupler and then redistributed at the two output ports as illustrated in figure 2.10.

To describe the physics of light wave coupling we start from a simple mathematical model regardless of the light coupling mechanism. Following the convention introduced in Chap. 1, we describe the time dependence of the light signals at the 4 ports as

$$E_n(t) = \frac{1}{2} E_n \exp(-i\omega t) + \text{c.c.} \tag{2.13}$$

where E_n ($n = 1,\ 2,\ 3,$ and 4) are the complex amplitudes of the electric fields, and c.c. stands for the complex conjugate.

For an ideal loss-less 2 × 2 coupler, the output is a unitary transformation of the input, which can be conveniently expressed in the form a unitary matrix U

$$\begin{bmatrix} E_3 \\ E_4 \end{bmatrix} = U \begin{bmatrix} E_1 \\ E_2 \end{bmatrix} = \begin{bmatrix} a & b \\ -b^* & a^* \end{bmatrix} \begin{bmatrix} E_1 \\ E_2 \end{bmatrix}. \tag{2.14}$$

Here, a and b are complex values (a^* and b^* are their complex conjugate), which satisfy the following normalization constraint

$$|a|^2 + |b|^2 = 1. \tag{2.15}$$

This unitary transformation guarantees that the total optical "power" is conserved (loss-less)

$$|E_3|^2 + |E_4|^2 = |E_1|^2 + |E_2|^2. \tag{2.16}$$

The values of $|a|^2$ and $|b|^2$, usually expressed in percentages, are the coupler's power splitting ratios for the parallel and cross paths. For example, a 50/50 coupler and an 80/20 coupler can be described with $U = \frac{1}{\sqrt{2}} \begin{bmatrix} 1 & 1 \\ -1 & 1 \end{bmatrix}$ and $U = \begin{bmatrix} \sqrt{0.8} & \sqrt{0.2} \\ -\sqrt{0.2} & \sqrt{0.8} \end{bmatrix}$, respectively.

People familiar with electron spin in quantum mechanics may recognize that matrix U has the same properties as a spin-1/2 rotation operator. It also resembles the Jones matrix for a loss-less polarization component (to be discussed in Sect. 2.4.5). In fact the underlying mathematics is very much the same for these distinctly different physical subjects (It would be an insightful exercise to expand matrix U in terms of the elegant Pauli matrices. But this is beyond the scope of this book and we leave it to the interested readers).

It should be noted that matrix U is not unique, and the same coupler may be described with other equivalent forms of U. For example, a 50/50 coupler could as well be represented by $U = \frac{1}{\sqrt{2}}\begin{bmatrix} 1 & 1 \\ 1 & -1 \end{bmatrix}$ or $U = \frac{1}{\sqrt{2}}\begin{bmatrix} 1 & i \\ i & 1 \end{bmatrix}$. Depending on the exact locations where the input and output amplitudes E_n ($n = 1,\ 2\ ,\ 3,$ and 4) are defined, the matrix U could absorb some additional phase factors. For instance, if E_4 for the 4th port is re-defined at a different location along the fiber such that E_4 has a phase shift of π or $E_4' = E_4 \exp(i\pi) = -E_4$, Eq. (2.14) can then be rewritten as

$$\begin{bmatrix} E_3 \\ E_4' \end{bmatrix} = \begin{bmatrix} E_3 \\ -E_4 \end{bmatrix} = \begin{bmatrix} 1 & 0 \\ 0 & -1 \end{bmatrix} \begin{bmatrix} a & b \\ -b^* & a^* \end{bmatrix} \begin{bmatrix} E_1 \\ E_2 \end{bmatrix} = \begin{bmatrix} a & b \\ b^* & -a^* \end{bmatrix} \begin{bmatrix} E_1 \\ E_2 \end{bmatrix}. \quad (2.17)$$

Note the transformation matrix has changed after absorbing a phase factor matrix. A global common phase factor has no significance in the analysis, but relative phases are critical for the interference outcome. It is very important to keep track of the phase factors in a consistent manner.

For non-monochromatic light waves, the ω-dependence of U must be considered. In general, all matrix elements of U vary with ω, not only the amplitude but also the phase. Variation of amplitudes $|a|$ and $|b|$ means the coupler splitting ratios are wavelength dependent. Variation of the phases, on the other hand, indicates time delay and group velocity dispersion.

2.4.2 Mach–Zehnder Interferometer

The matrix representation is very convenient for the analysis of a fiber optic interferometric system. Figure 2.11 shows a simple layout of a Mach–Zehnder interferometer containing two 50/50 couplers and a phase shift element in between

As discussed earlier, the two 50/50 couplers can be described with

$$U_1 = U_3 = \frac{1}{\sqrt{2}}\begin{bmatrix} 1 & 1 \\ 1 & -1 \end{bmatrix} \quad (2.18)$$

The phase shifter in the middle section is represented by a diagonal matrix:

$$U_2 = \begin{bmatrix} \exp(i\phi) & 0 \\ 0 & 1 \end{bmatrix}. \quad (2.19)$$

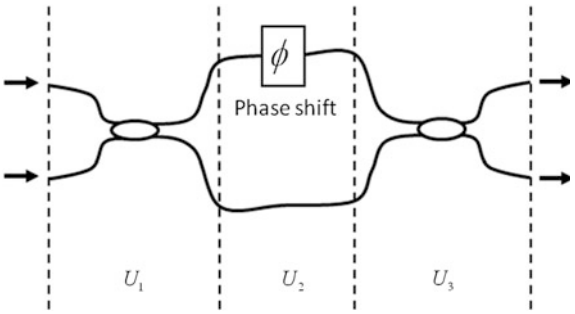

Fig. 2.11 Mach-Zehnder interferometer comprising 3 segments described by unitary matrices U_1, U_2, and U_3

For convenience we multiply a common phase factor $\exp(-i\phi/2)$ and express U_2 in a more symmetric form (only the relative phase matters)

$$U_2 = \begin{bmatrix} e^{i\phi/2} & 0 \\ 0 & e^{-i\phi/2} \end{bmatrix}. \tag{2.20}$$

The overall transformation matrix for the entire system can then be computed by concatenating the three matrices

$$\begin{aligned} U_{\text{total}} = U_3U_2U_1 &= \left(\frac{1}{\sqrt{2}}\right)^2 \begin{bmatrix} 1 & 1 \\ 1 & -1 \end{bmatrix} \begin{bmatrix} e^{i\phi/2} & 0 \\ 0 & e^{-i\phi/2} \end{bmatrix} \begin{bmatrix} 1 & 1 \\ 1 & -1 \end{bmatrix} \\ &= \frac{1}{2} \begin{bmatrix} e^{i\phi/2} + e^{-i\phi/2} & e^{i\phi/2} - e^{-i\phi/2} \\ e^{i\phi/2} - e^{-i\phi/2} & e^{i\phi/2} + e^{-i\phi/2} \end{bmatrix} = \begin{bmatrix} \cos(\phi/2) & i\sin(\phi/2) \\ i\sin(\phi/2) & \cos(\phi/2) \end{bmatrix} \end{aligned} \tag{2.21}$$

This result indicates that the system behaves like an optical switch. When $\phi = 0$ the resulting matrix $U_{\text{total}} = \begin{bmatrix} 1 & 0 \\ 0 & 1 \end{bmatrix}$ represents a 100 % parallel-state, and when $\phi = \pi$ the resulting matrix $U_{\text{total}} = \begin{bmatrix} 0 & i \\ i & 0 \end{bmatrix}$ represents a 100 % cross-state.

2.4.3 Michelson Interferometer

In Sect. 2.3.1 we have also introduced an important interferometer topology, the Michelson interferometer, which involves reflecting the two output signals of the 2×2 coupler back into the same coupler to achieve optical interference (Fig. 2.5). To model such an interferometer, it is necessary to know the transformation matrix of the same coupler for light waves propagating in the opposite

direction (input at ports 3 and 4, and output at ports 1 and 2 in Fig. 2.10). In the following, we show that the matrix for the reverse propagating light is U^T, the transpose of U. In some sense this is a trivial result: it simply means the matrix element that links a specific input port to a specific output port is reciprocal and remains the same regardless of light transmission direction.

The derivation is based on time reversal symmetry, which the ideal loss-less 2×2 fiber optic coupler obeys. (Not all optical components obey time reversal symmetry, as will be discussed later in Sect. 2.4.6). By definition the unitary matrix U has the property $U^{-1} = U^+$ ("U dagger", conjugate transpose of U), Eq. (2.14) can be easily reversed

$$\begin{bmatrix} E_1 \\ E_2 \end{bmatrix} = U^+ \begin{bmatrix} E_3 \\ E_4 \end{bmatrix} = \begin{bmatrix} a^* & -b \\ b^* & a \end{bmatrix} \begin{bmatrix} E_3 \\ E_4 \end{bmatrix}. \tag{2.22}$$

But U^+ is not the matrix for the reverse propagating light waves. There is one extra step. Time reversal means replacing t with $-t$, and Eq. (2.13) becomes

$$\begin{aligned} E_n(-t) &= \frac{1}{2} E_n \exp[-i\omega(-t)] + \text{c.c.} \\ &= \frac{1}{2} E_n^* \exp(-i\omega t) + \text{c.c.} \end{aligned} \tag{2.23}$$

This means under time reversal, the complex amplitudes E_n ($n = 1,\ 2\ ,\ 3,$ and 4) all need to be replaced with their complex conjugate. Applying complex conjugate to both sides of Eq. (2.22), we have

$$\begin{bmatrix} E_1^* \\ E_2^* \end{bmatrix} = U^T \begin{bmatrix} E_3^* \\ E_4^* \end{bmatrix} = \begin{bmatrix} a & -b^* \\ b & a^* \end{bmatrix} \begin{bmatrix} E_3^* \\ E_4^* \end{bmatrix}. \tag{2.24}$$

This subtle difference between U^+ and U^T should not be overlooked. For example, let us consider a Michelson interferometer with perfectly reflective mirrors at ports 3 and 4. What is the overall transformation U_{total} after the light waves are reflected back into the coupler, interfere, and reemerge at ports 1 and 2. Knowing the transformation in the reverse direction is U^T, we can perform a straightforward calculation (ignoring a common phase factor introduced by the mirrors):

$$U_{\text{total}} = U^T U = \begin{bmatrix} a & -b^* \\ b & a^* \end{bmatrix} \begin{bmatrix} a & b \\ -b^* & a^* \end{bmatrix} = \begin{bmatrix} a^2 + b^{*2} & ab - a^* b^* \\ ab - a^* b^* & a^{*2} + b^2 \end{bmatrix}. \tag{2.25}$$

If U^+ were used instead of U^T for the counter-propagating waves, the answer would be a unit matrix regardless of the nature of the coupler, which is obviously incorrect.

2.4.4 Other Fiber Optic Couplers

The loss-less 2 × 2 coupler discussed so far is only an ideal physical model. In reality, couplers all have finite optical losses. More realistic 2 × 2 couplers can be modeled using an ideal 2 × 2 coupler by adding attenuations to individual ports. Once the attenuation is included, the transformation matrix U is no longer unitary and some of the symmetry properties of an ideal 2 × 2 coupler no longer exist. For a realistic 2 × 2 coupler in general, the coupling ratios for the two through paths (from port 1 to port 3 and from port 2 to port 4) can be different. So are the coupling ratios for the two cross paths (from port 1 to port 4 and from port 2 to port 3). Nevertheless, one can often still use Eq. (2.14) as an approximation for a lossy 2 × 2 coupler by lowering the value of $|a|^2 + |b|^2$ to below 1. The value of $-10\log\left(|a|^2 + |b|^2\right)$ is called the "excess loss" (in dB) of the coupler. The excess loss of a good quality fiber optic coupler is typically less than 0.1 dB.

There are other kinds of fiber optic couplers such as a 1 × 2 Y-coupler or a more sophisticated 3 × 3 coupler. A 1 × 2 Y-coupler can be simply modeled with a 2 × 2 coupler having one of the 4 ports not used (terminated with an index-matching absorber). An ideal 3 × 3 coupler, on the other hand, could be modeled theoretically with a 3 × 3 unitary matrix. A 3 × 3 coupler is more difficult to fabricate and it is not nearly as common as the 2 × 2 coupler in fiber optic interferometry.

2.4.5 Fiber Birefringence and Polarization Controllers

The polarization effect has been ignored in the theoretical model presented above. As we mentioned earlier, the "single-mode" fiber actually supports two degenerate modes of orthogonal polarizations. For a realistic interferometric system based on single mode fibers, the two polarization modes must be considered and polarization controllers are frequently used.

As we take into account the effect of polarization, a simple section of optical fiber itself becomes a 2 × 2 coupler. Fiber birefringence causes coupling between the two polarization modes in a way very similar to light wave coupling in a 2 × 2 coupler discussed in the previous section. When polarization is considered, a 2 × 2 fiber optic coupler in some sense becomes a 4 × 4 coupler and the transformation matrices will have to be expanded.

The polarization state of light in a single-mode optical fiber is very similar to that of a plane light wave in free space. It could be linear, circular, or elliptical. In the following, we shall briefly describe the mathematical tools for modeling polarization. We do not intend to go into all the details of polarization optics since they are not the focus of this book. There are many good text books on this subject, for example [2, 3].

To model polarization, we first define two orthogonal polarization states along the fiber as the basis vectors. These two polarizations do not have to be linear, although linear polarizations are often chosen for convenience. Once the basis polarization states are defined, the electric field of the light is projected to these two basis vectors, resulting in two complex amplitudes E_x and E_y (we use subscripts "x" and "y" here assuming horizontal and vertical linear polarizations are the chosen basis). The complex vector $\begin{bmatrix} E_x \\ E_y \end{bmatrix}$ is called the Jones vector.

Since a complex number has a real part and an imaginary part, a Jones vector contains total 4 independent parameters. The polarization information is actually fully described by just 2 independent parameters (a point on the 2-dimensional surface of the Poincare sphere). The other 2 independent parameters in the Jones vector are the magnitude $\sqrt{|E_x|^2 + |E_y|^2}$ and a common phase, which can be factored out if we are interested in the polarization only.

As light travels through a fiber optic system, the Jones vector is transformed by a 2×2 matrix known as the Jones matrix

$$\begin{bmatrix} E_{2x} \\ E_{2y} \end{bmatrix} = J \begin{bmatrix} E_{1x} \\ E_{1y} \end{bmatrix} = \begin{bmatrix} J_{xx} & J_{xy} \\ J_{yx} & J_{yy} \end{bmatrix} \begin{bmatrix} E_{1x} \\ E_{1y} \end{bmatrix}. \tag{2.26}$$

Note the similarity of Jones matrix J to the U matrix for the ideal 2×2 fiber optic coupler discussed in Sect. 2.4.1. In fact, for a non-absorbing (loss-less) polarization control device (a wave plate, for example), J is also a unitary matrix and it takes the same general form as described in Eq. (2.14). Regardless of the construction of the device, a unitary Jones matrix always has two orthogonal eigenvectors with two phase-only eigenvalues (norm = 1). These two eigenvectors correspond to two principal optical "axes" (generalized to include circular and elliptical polarizations), which do not change during the transformation. The two eigenvalues determine the phase retardation between the two optical axes. Therefore, any non-absorbing polarization control device can be generally considered a phase retarder.

The most commonly used fiber optic polarization controller is realized by bending the single-mode fiber into a loop (it could also be partial or multiple loops). Bending induces birefringence through anisotropic stress at the fiber core. Alternatively, one can apply anisotropic pressure on a section of fiber without bending to achieve similar effects. By symmetry, the optical axes are the two directions parallel and perpendicular to the plane of the loop. The amount of phase retardation of a fiber loop is inversely proportional to the loop diameter: the smaller the diameter, the higher the phase retardation. The Jones matrix of such a fiber loop oriented at angle θ with a phase retardation of δ is

$$J = \begin{bmatrix} \cos\frac{\delta}{2} + i\sin\frac{\delta}{2}\cos 2\theta & i\sin\frac{\delta}{2}\sin 2\theta \\ i\sin\frac{\delta}{2}\sin 2\theta & \cos\frac{\delta}{2} - i\sin\frac{\delta}{2}\cos 2\theta \end{bmatrix}. \tag{2.27}$$

For example, a fiber loop oriented at a 45° angle between horizontal and vertical ($\theta = \pi/4$) with a phase retardation $\delta = \pi/2$ (equivalent to a $\lambda/4$ waveplate) has the following Jones matrix

$$J = \begin{bmatrix} \cos\frac{\pi}{4} + i\sin\frac{\pi}{4}\cos\frac{\pi}{2} & i\sin\frac{\pi}{4}\sin\frac{\pi}{2} \\ i\sin\frac{\pi}{4}\sin\frac{\pi}{2} & \cos\frac{\pi}{4} - i\sin\frac{\pi}{4}\cos\frac{\pi}{2} \end{bmatrix} = \frac{1}{\sqrt{2}}\begin{bmatrix} 1 & i \\ i & 1 \end{bmatrix}. \tag{2.28}$$

Consider a horizontally polarized light input $\begin{bmatrix} E_{1x} \\ E_{1y} \end{bmatrix} = \begin{bmatrix} 1 \\ 0 \end{bmatrix}$, after passing this $\lambda/4$ waveplate, the output becomes circularly polarized

$$\begin{bmatrix} E_{2x} \\ E_{2y} \end{bmatrix} = \frac{1}{\sqrt{2}}\begin{bmatrix} 1 & i \\ i & 1 \end{bmatrix}\begin{bmatrix} 1 \\ 0 \end{bmatrix} = \frac{1}{\sqrt{2}}\begin{bmatrix} 1 \\ i \end{bmatrix}. \tag{2.29}$$

A manual fiber optic polarization controller usually consists of 2 or 3 fiber loops with different diameters and adjustable orientations. The total effect can be modeled by multiplying the Jones matrices of the individual fiber loops, each being a linear waveplate. Excluding a common phase factor, any non-absorbing polarization controller has only 3 independent parameters (3 degrees of freedom): 2 for defining the principal optical axes, and 1 for the retardation. In principle, a polarization controller consisting of 3 fiber loops is sufficient to produce any desired Jones matrix for polarization adjustment.

Again, similar to the ideal 2 × 2 fiber optic coupler, non-absorbing polarization devices based on mechanical stress induced birefringence obey time reversal symmetry. As a result, the Jones matrices for the forward and backward directions are the transpose of each other.

Although much of the discussion in this section is about non-absorbing polarization devices, the Jones matrix is also used to describe polarization components that do absorb light. For example, a polarizer that blocks vertically polarized light but passes horizontally polarized light can be described by a non-unitary Jones matrix

$$\begin{bmatrix} E_{2x} \\ E_{2y} \end{bmatrix} = J\begin{bmatrix} E_{1x} \\ E_{1y} \end{bmatrix} = \begin{bmatrix} 1 & 0 \\ 0 & 0 \end{bmatrix}\begin{bmatrix} E_{1x} \\ E_{1y} \end{bmatrix}. \tag{2.30}$$

2.4.6 Fiber Optic Circulators and Isolators

The fiber optic circulator is an interesting and very useful device. A typical circulator has 3 ports and the light wave propagates in a circular fashion as shown in Fig. 2.12

Such a device is non-reciprocal. It appears to violate time reversal symmetry: the light path from port 1 to port 2 can be theoretically loss-less and yet it is unidirectional and irreversible. There are different designs for optical circulators, and all of them involve the non-reciprocal property of Faraday effect.

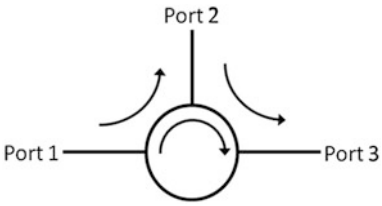

Fig. 2.12 Three-port optical circulator

The Faraday effect is a magneto-optic effect, in which the polarization of light is rotated in an optical medium with a magnetic field applied along the light propagation direction (Fig. 2.13).

Polarization rotation can also occur without magnetic field. The general effect is called optical activity, for example, in crystalline quartz that exhibits chirality. Optical activity causes the refractive indices for right-hand and left-hand circularly polarized light waves to differ. The Faraday effect can be viewed as optical activity induced by magnetic field. However, there is a fundamental difference between the Faraday effect and optical activity caused by chirality. In the absence of magnetic field, optical activity is reciprocal: when light transmission direction is reversed, so is the polarization rotation. The Faraday effect, on the other hand, is non-reciprocal: the polarization rotates in the same direction regardless of the light transmission direction. The time reversal symmetry is not really violated because the magnetic field must flip its direction in a truly time-reversed world.

This peculiar property of Faraday effect makes optical circulator possible. Figure 2.14 shows one possible way to construct an optical circulator.

It contains two polarization splitters/combiners, a half-waveplate, and a Faraday rotator. The optical axis of the half-waveplate is at 22.5° from the x-axis, and it rotates the both x and y polarizations by 45° in a reciprocal manner. The Faraday rotator, on the other hand, also produces a 45° rotation, but non-reciprocal. As a result, in one direction (Fig. 2.14, schematic on the left), when light passes both the half-waveplate and the Faraday rotator, the polarization is unchanged. But in

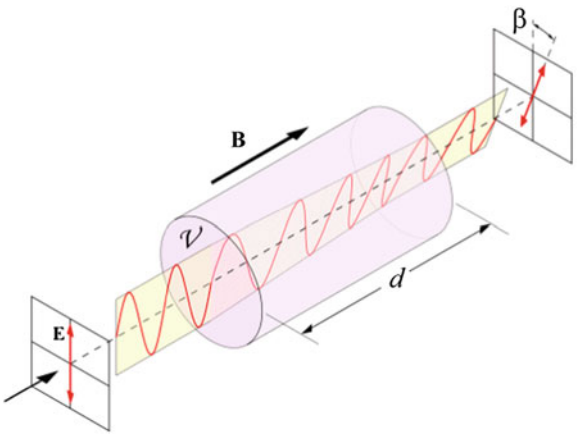

Fig. 2.13 Rotation of light polarization due to the Faraday effect [Image courtesy: Wikimedia commons image file database (drawing by: Bob Mellish)]

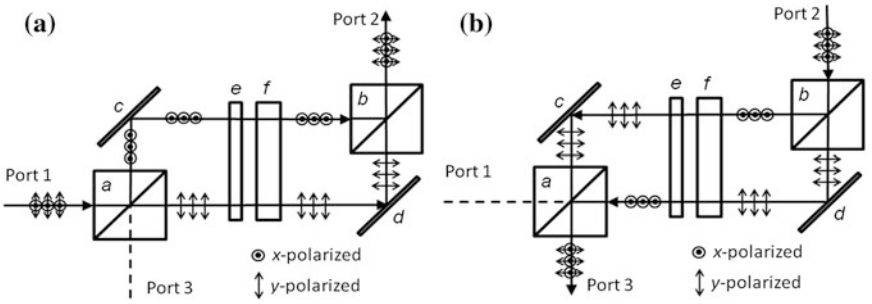

Fig. 2.14 Non-reciprocal light propagation based on Faraday rotation: (*a*) and (*b*) polarization beam splitters/combiners, (*c*) and (*d*) mirrors, (*e*) half-waveplate, and (*f*) Faraday rotator

the opposite direction (Fig. 2.14, schematic on the right), the polarization is rotated by 90°. Therefore, in the forward direction light travels from port 1 to port 2, but in the backward direction light entering port 2 would come out at port 3.

A fiber optic isolator is a simpler device with only two ports, and it is based on the same operation principle as the circulator. Light can travel in one direction but not the other. An optical isolator is often used to prevent back-reflection that tends to cause light source instability and degradation.

2.5 Conclusion

Fiber optic interferometric sensors have found several industrial applications including fiber optic gyros for navigation in airplanes and space-based systems, high-precision process control and manufacturing, structural health monitoring of bridges, dams, ships etc., oil and gas exploration activities, medical applications and so on.

While the sensitivity of the fiber optic interferometric sensors is typically very high, an important challenge lies in the capability to differentiate the environmental perturbations such as temperature, strain, pressure etc. In principle, all environmental perturbations could be converted to optical signals by applying appropriate transducing mechanisms. However, sometimes multiple effects could contribute simultaneously and modify the light in the fiber in a similar manner. For example, changes in temperature, strain, pressure or any mechanical perturbation could all impact the light in fiber by changing fiber lengths and refractive index such that it is difficult to differentiate one perturbation to another. The right solution to such challenges is the design of appropriate transducing mechanism that is selective in nature towards the measurement of a desired environmental perturbation.

Although the fiber optic sensors have already proven superior performances, their relatively higher cost compared to conventional low cost sensors remains a barrier towards its widespread adoption for wider range of applications. The semiconductor industry has continued to progress steadily over the last few

decades and as a result we have seen steady decrease in the cost of laser diodes, detectors and other optoelectronic devices. It is expected that the further decrease in optoelectronic components cost in future could be the right catalyst for the continued progress of this field.

References

1. Born M, Wolf E (1999) Principles of optics, 7th edn. Cambridge University Press, Cambridge
2. Hecht E (2002) Optics, 4th edn. Addison Wesley, San Francisco
3. Saleh BEA, Teich MC (1991) Fundamentals of photonics. Wiley Interscience, New York
4. Udd E (1991) Fiber Optic Sensors. Wiley Interscience, New York
5. Udd E, Spillman Jr WB (2011) Fiber optic sensors: an introduction for engineers and scientists, 2nd edn. Wiley, New York
6. Culshaw B (2008) Fiber-optic sensing: a historical perspective. J Lightwave Technol 26(9):1064–1078

http://www.springer.com/978-1-4614-7481-4

Fiber Optic Sensing and Imaging
Kang, J.U. (Ed.)
2013, VII, 171 p. 124 illus., 70 illus. in color., Hardcover
ISBN: 978-1-4614-7481-4